Journal of Hydrology 567 (2018) 420–434

Contents lists available at ScienceDirect

Journal of Hydrology

journal homepage: www.elsevier.com/locate/jhydrol

Research papers

Modeling impacts of climate change on return period of landslide triggering

D.J. Peres*, A. Cancelliere

Department of Civil Engineering and Architecture, University of Catania, Via Santa Sofia, 64, 95123 Catania, Italy

ARTICLE INFO

This manuscript was handled by Marco Borga, Editor-in-Chief, with the assistance of Yu Zhang, Associate Editor

Keywords:
Landslides
Stochastic models
Climate Change
Monte Carlo simulation
Regional climate models

ABSTRACT

Quantifying the potential influence of climate change on future landslide hazard requires methodologies that allow to properly take into account nonstationarities in the hydro-meteorological causes.

In this paper we provide a methodology for estimating return period of landslide triggering under climate change.

The methodology capitalizes on the combined use of a stochastic rainfall generator and a hydrological and slope stability model. The stochastic rainfall generator takes into account the statistical dependency between rainfall event duration and intensity through copulas. The hydrological model is based on an analytical solution of a simplified version of the Richards vertical infiltration equation and slope stability is assessed by the infinite slope model. The combined model enables to estimate landslide probability through Monte Carlo simulations. Climate change is then introduced by perturbing the parameters of the rainfall stochastic generator based on factors of change derived from the comparison of future scenarios and the baseline climate as simulated by Regional climate models (RCMs). The Monte Carlo simulations are conducted sequentially on a future moving time window, to derive a yearly series of future landslide triggering probability. This series is then used to compute landslide return period by formulas suitable under nonstationary conditions.

An application to the landslide prone region of the Peloritani Mountains, Southern Italy, is carried out to demonstrate the proposed approach. For the application, climate change projections of three RCMs of the MED-CORDEX initiative are used, and a preliminary assessment of the impacts of intermediate- and high-emission Representative concentration pathways (RCPs) 4.5 and 8.5 is carried out.

1. Introduction

Landslides are a natural phenomenon shaping the Earth's surface and a hazard globally provoking hundreds of deaths every year (Sidle and Ochiai, 2006; Froude and Petley, 2018).

Landslide processes are typically nonstationary, at both intra-annual (seasonality) and inter-annual time scales. Sidle and Ochiai (2006) describe most of nonstationary processes of interest in the study of landslides, which include reactivation processes, land use modifications, and climatic changes. The latter are expected to modify meteorological conditions and to have significant impacts on landslides and other hydrological hazards (IPCC, 2014).

Since the late 1990s an increasing number of papers focused on the assessment of the potential effects of climate change on landslide phenomena, based on three distinct approaches (Gariano and Guzzetti, 2016, and references therein): modeling approaches, historical analyses, and identification of paleo-landslide evidences. The first consist in assessing the impacts of climate change on a given phenomenon, based on climate projections from Global circulation models (GCMs) and derived downscaled climatic products. GCMs simulate the effects on climate of emission scenarios defined by international programs (Taylor et al., 2012), and better known as Representative concentration pathways (RCPs) (briefly "scenarios" in the ensuing text). Regional climate models (RCMs) provide higher resolution data (up to 10–20 km or less), as a result of dynamical downscaling of GCM data having a coarser resolution (250–600 km). Commonly, modeling approaches couple these climate model simulations with empirical or physically based models providing triggering conditions as a more or less explicit function of climatic variables – mainly precipitation (Ciabatta et al., 2016; Rianna et al., 2016; Gariano et al., 2017; Alvioli et al., 2018).

Climate change studies led to contrasting conclusions on whether an increase or a decrease should be expected in landslide frequency in the future (Crozier, 2010; Coe and Godt, 2012). The high level of uncertainty is substantially confirmed by IPCC special report of Seneviratne et al. (2012), which indicates a "variable level of confidence" for an increase of landslide activity in the future, opening an implicit request for further studies.

Notwithstanding an increasing literature focused on the assessment

* Corresponding author.
E-mail address: djperes@dica.unict.it (D.J. Peres).

https://doi.org/10.1016/j.jhydrol.2018.10.036
Received 5 June 2018; Received in revised form 4 September 2018; Accepted 18 October 2018
Available online 19 October 2018

of climate change impacts on landslides, there is a lack of studies focusing on the possible changes on landslide return period, a widely-used metric to express landslide hazard, useful in designing mitigation infrastructures (Borga et al., 2002; D'Odorico et al., 2005; Rosso et al., 2006; Simoni et al., 2008; Salciarini et al., 2008; Tarolli et al., 2011; Peres and Cancelliere, 2016). The need to address this aim derives also from the fact that the concept of return period has been recently revisited to take into account nonstationary processes (Salas and Obeysekera, 2014; Obeysekera and Salas, 2016; Cancelliere, 2017), which change the way return period is estimated, because landslide probability varies in time. This paper aims at addressing this issue, proposing a modeling approach for estimating return period of landslide triggering under a changing climate, taking into account the induced nonstationarities in precipitation. To this aim, we use RCM products within a Monte Carlo simulation approach (Peres and Cancelliere, 2014; Peres and Cancelliere, 2016). The Monte Carlo simulation scheme is herein based on the combined use of a stochastic rainfall generator and a hydrological and slope stability model. A single Monte Carlo simulation yields an estimate of landslide probability for a given climate. By perturbing the stochastic rainfall model based on RCM projections, a series of future landslide probabilities can be derived. Perturbation is here based factor of changes of rainfall event statistical properties (Kilsby et al., 2007; Anandhi et al., 2011; Fatichi et al., 2011; Maraun et al., 2010; Teutschbein and Seibert, 2012; Ehret et al., 2012). Finally, return period is computed, as a function of the estimated future landslide probability series, according to nonstationary formulations provided by Salas and Obeysekera (2014).

The stochastic rainfall generator we devise takes into account of the statistical dependence between rainfall event duration and intensity, thanks to a copula approach. The hydrological and slope stability model is based on the diffusive infiltration model introduced by Iverson (2000) extended to a finite soil depth (Baum et al., 2002), and simplified to the computation of peak pressure head response to rainfall events, allowing a more efficient application than other software implementations (Baum et al., 2010; Alvioli and Baum, 2016) that constrain the user to compute the complete response to rainfall time-series.

An application of the methodology is carried out with reference to the Peloritani mountains in Sicily, an area that has experienced several landslides in the recent decades. The application exercise allows to test the suitability of the methodology in real-world situations; the specific results obtained also offer a preliminary assessment of the potential impacts of climate change on landslide activity in this area. The application is conduced for three different RCM products of the MED-CORDEX initiative, so a measure of the spread related to RCM uncertainties is also provided.

2. Methodology

2.1. Return period in a nonstationary context

Return period can be rigorously defined by introducing random variate Y as the time at which a given critical event (slope instability, in our case) occurs for the first time.

In the stationary case, probability of the phenomena is constant in time, say equal to p_0. It can be shown that the probability that a critical event occurs for the first time at year y is given by the geometric distribution law (Mood et al., 1974):

$$f(y) = (1 - p_0)^{y-1} p_0, \quad y = 1, 2, \ldots; \tag{1}$$

thus return period $\mathcal{T}_0$, which can be defined as the mean number of years that will take for the first occurrence of a critical event, is given by the well-known formula (Chow et al., 1988):

$$\mathcal{T}_0 = E(Y) = \frac{1}{p_0}. \tag{2}$$

In the nonstationary case, critical event probability varies in time. If we denote as p_y that probability at time y, it has been shown by Salas and Obeysekera (2014) that

$$f(y) = p_y \prod_{t=1}^{y-1} (1 - p_t) \quad \text{with } y = 1, 2, \ldots, \infty; \tag{3}$$

thus, return period becomes:

$$\mathcal{T}_0 = E(Y) = \sum_{y=1}^{\infty} y f(y) = \sum_{y=1}^{\infty} y p_y \prod_{t=1}^{y-1} (1 - p_t). \tag{4}$$

This equation can be generalized to compute return period at a given time, by introducing an additional time variate, ν, which is the time at which one desires to estimate return period:

$$\mathcal{T}_\nu = \sum_{y=1}^{\infty} y p_{\nu+y-1} \prod_{t=1}^{y-1} (1 - p_{\nu+t-1}). \tag{5}$$

All formulas above require just the estimation of the landslide probability series, which is here carried out via Monte Carlo simulations.

2.2. Computation of landslide probability

In our approach each Monte Carlo simulation allows to compute landslide probability for a given climate. As already mentioned, the simulation consist in the combination a stochastic rainfall generator and a physically based model, by which a long virtual synthetic series of rainfall and landslide response can be obtained.

Let us denote with M the length of a Monte Carlo simulation in (virtual) years. Provided that M is sufficiently large, landslide probability can be estimated frequentistically as:

$$p = \frac{1}{M} \sum_{m=1}^{M} I_m \tag{6}$$

where

$$I_m = \begin{cases} 1, & \text{if in virtual year } m \text{ at least a landslide occurred} \\ 0, & \text{otherwise} \end{cases} \tag{7}$$

In the Monte Carlo modeling we assume that a landslide occurs each time the factor of safety F_S for slope stability drops down to 1. Here we work under the assumption of an infinite slope, for which:

$$F_S = \frac{\tan\phi'}{\tan\delta} + \frac{c' - \psi(d_{LZ}, t_p)\gamma_w \tan\phi'}{\gamma_s d_{LZ} \sin\delta \cos\delta} \tag{8}$$

where ϕ' is friction angle, c' is soil cohesion, δ is terrain slope, $\gamma_w = 9800$ N/m^3 is the unit weight of water, γ_s the unit weight of soil, d_{LZ} is soil depth, $\psi(t_p, d_{LZ})$ is pressure head at the peak time t_p measured from rainfall event start (see Section 2.4) and at soil depth $Z = d_{LZ}$. This is equivalent to comparing peak pressure head with a critical value ψ_{CR}, which is obtained by rearranging the above equation and letting $F_S = 1$:

$$\psi_{CR} = \frac{c'}{\gamma_w \tan\phi'} - \frac{\gamma_s d_{LZ} \sin\delta \cos\delta}{\gamma_w \tan\phi'} \left(1 - \frac{\tan\phi'}{\tan\delta}\right). \tag{9}$$

Though more sophisticated and accurate three-dimensional slope stability models have been recently proposed (Lehmann and Or, 2012; Milledge et al., 2014; Bellugi et al., 2015; Reid et al., 2015), the infinite slope stability analysis remains still reliable for a first-stage assessment of landslide triggering hazard (Baum et al., 2010; Arnone et al., 2011; Raia et al., 2014; Capparelli and Versace, 2014).

Pressure head needed to be compared with ψ_{CR} can be estimated from any suitable hydrological model. Herein we use a model based on the diffusive infiltration model proposed by Iverson (2000), extended for a finite soil depth (Baum et al., 2002), and a linear reservoir drainage model that acts within dry intervals (Peres and Cancelliere, 2014), as described more in detail in Section 2.4. We proceed in a lumped fashion, i.e. model the response of the area of interest by a single set of

geomorphological, hydrological and geotechnical parameters, which are globally representative of slopes subject to landslides in the area of interest. To test the suitability of the lumped model in the given region of interest, it is checked if it reproduces landslides occurrence dates in the region for the period covered by the observed record (see Section 3). In this sense, this lumped approach is similar to empirical landslide-triggering thresholds (Caine, 1980; Guzzetti et al., 2008; Greco et al., 2013; Peruccacci et al., 2017; Peres et al., 2018), where a single relationship is used to establish whether or not a given rainfall event will trigger landslides in a region. Here, instead of using an empirical relationship, we use a lumped approach that has a physically-based rationale, following recent perspectives on landslide research (Bogaard and Greco, 2018).

The input to the hydrological model is provided by the stochastic rainfall model, which is also able to take into account climatic changes. Stochastic rainfall generators can be of a very wide degree of complexity, and are mostly all suitable to take into account climate change scenarios, as simulated by RCMs, by means of a factor of changes approach (Fatichi et al., 2011; Kilsby et al., 2007). For our purpose we have devised a specific rainfall event sequences generator based on copulas, described more in detail in Section 2.3. We just anticipate here that respect to other stochastic models presented in the literature, the one we propose here has the advantage to allow parameter adjustment simply from the statistical moments of rainfall characteristics, namely event duration T, total depth H and the no-rain time separating one event from another (interarrival time) U. In a climate change context, a control and a future period are distinguished. For the control period both the historical RCM simulation and observed data may be available, while only the former is for the future climate referred to year ν. If $\mathcal{M}_C^{RCM}$ and $\mathcal{M}_\nu^{RCM}$ are the statistical moments computed from RCM in the control and future period, respectively, then the factor of change for moment $\mathcal{M}$ is given by the ratio:

$$\mathcal{F}_\nu = \frac{\mathcal{M}_\nu^{RCM}}{\mathcal{M}_C^{RCM}}, \tag{10}$$

The factor of change can be used to estimate the future value of the moment $\mathcal{M}_\nu$, by multiplication to the observed moment in the control period $\mathcal{M}_C^{OBS}$:

$$\mathcal{M}_\nu = \mathcal{M}_C^{OBS}\mathcal{F}_\nu \tag{11}$$

The moments obtained from Eq. (11) are then plugged into the method of moments parameter estimators (MME), by which the corrected parameters of the stochastic model for future periods are obtained. In order to apply Eqs. (10) and (11) the spatial inconsistency between RCM data and observations should be resolved, for instance by interpolation. To this aim we have interpreted the RCM data as relative to the center of the grid cells. Thus, the interpolation averages the RCM data as a function of the distance of the grid cell centers to the observation point (rain gauge). This way to proceed preserves the temporal structure of the observed rainfall time series.

Landslide return period for the control period, is obtained by Monte Carlo simulation with the stochastic model calibrated on observed rainfall data, and application of Eqs. (6), (7) and (2). RCMs provide scenarios for the years 2005–2100. Within this period we define, on a yearly-moving time window, sixty-one climatic periods thirty-years long: first period $\nu = 1$ corresponds to years 2011–2040, $\nu = 2$ to years 2012–2041, and so on, until the last period 2061–2100 ($\nu = 61$) is reached. Hence, for each future scenario landslide probability p_ν can be computed, $\nu = 1, 2, \ldots, 61$. This series of probabilities is then plugged in Eq. (5) to compute the return period sequence. For this purpose we assume that for $\nu > 61$, $p_\nu = p_{61}$.

Fig. 1 summarizes the main steps and features of the proposed methodology.

2.3. Stochastic point rainfall event generator based on copulas

Stochastic rainfall point models allow simulation of rainfall time series at a given location (Salas, 1993). The resulting generated rainfall sequences reproduce the statistical features of the observed series which are significant for the problem at hand. The main advantage of using a stochastic model is that synthetic series can have a virtually unlimited length, allowing to estimate landslide probability based on the frequentist definition – see Eqs. (6) and (7).

Here we devise a specific point stochastic model for the generation of sequences of rectangular rainfall events with statistical dependence between their total depth H and duration T, modeled through copula functions (Nelsen, 2007). The importance to take into account such dependence has been highlighted by different studies (e.g. De Michele et al., 2003; Evin and Favre, 2008; Vernieuwe et al., 2015), and it is desirable within landslide modeling, given the high number of studies linking the occurrence of this phenomenon to event rainfall duration and mean intensity (Sidle and Ochiai, 2006; Guzzetti et al., 2007; Peruccacci et al., 2017).

Specifically, the model is structured as follows (see Fig. 2):

- Event duration T and rainfall depth H are generated by a suitable bivariate model, to take into account their statistical dependence. The bivariate model is built using copula functions, that allow almost unconstrained choice of marginal distributions, F_T and F_H, of the two variables under investigation.
- Rainfall events are separated by dry intervals. These intervals are generated according to a suitable continuous probability distribution F_U.

In order to calibrate the model, given an observed time series, rainfall events have to be isolated with some criterion. Here a part of the rainfall time series is assumed to be a rainfall event when bounded by zero-rain (dry) periods of at least U_{min} hours long. The same procedure is applied to the RCM series as well. The choice of U_{min} may depend on the climatic features of the investigated area (Vessia et al., 2014; Melillo et al., 2015; Melillo et al., 2018).

We then fit marginal distributions to the series of observed rainfall events by using method-of-moments estimators (MME) of the distribution parameters. MME has the advantage to allow for easy adjustment of the stochastic model parameters, since change factors of only few moments of the RCM-derived rainfall event series are needed. The choice of marginal distributions can be guided by statistical hypothesis testing (D'Agostino and Stephens, 1986).

We apply the factor of changes adjustment, for generation of rainfall sequences in the climate change scenarios, only to the marginal distributions. The $H - T$ dependence (copula) parameters are not adjusted for the scenario periods. This has the advantage of model simplicity, since, otherwise, with a changing dependence structure, the specific parametric copulas suitable for the observational period may not be valid for the future periods. Nevertheless, changing marginals induce by themselves a modification of the $H - T$ bivariate distribution. Even if analytical goodness-of-fit tests are available in the literature (Genest et al., 2009), a simple and reliable method to check the suitability of a copula model is to compare the observed pairs with those randomly generated from the fitted copula (Genest and Favre, 2007). This approach is followed in several studies (e.g. Gyasi-Agyei and Melching, 2012; Callau Poduje and Haberlandt, 2017), and in this work as well (see Section 3.2).

2.4. Hydrological model of infiltration and drainage

The hydrological infiltration model we adopt is based on the model presented by Iverson (2000) extended to the case of a finite soil depth (Baum et al., 2002), and integrated with a water table recession model to compute the initial conditions at each rainfall event as an implicit

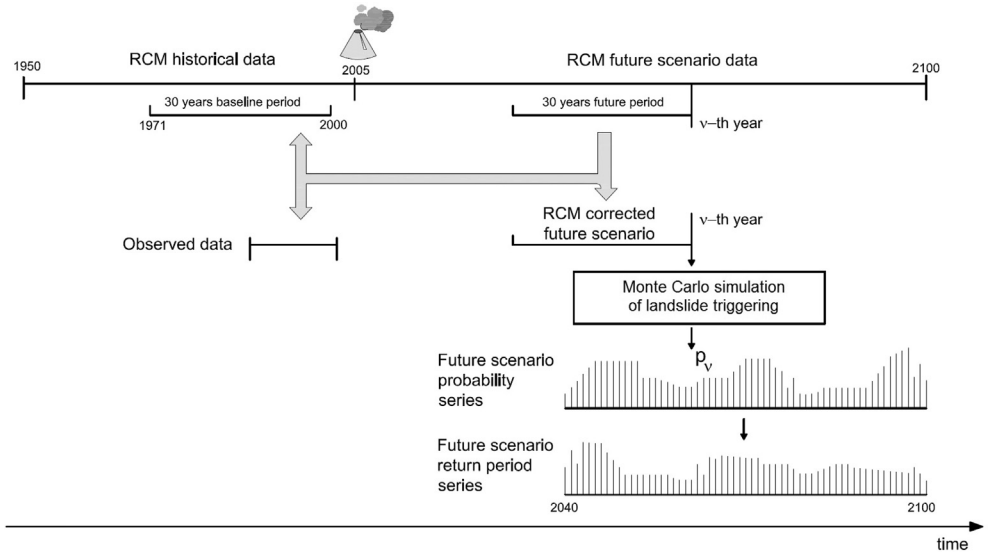

Fig. 1. Schematic depicting main steps of the proposed methodology for estimating landslide return period based on RCMs and Monte Carlo simulations.

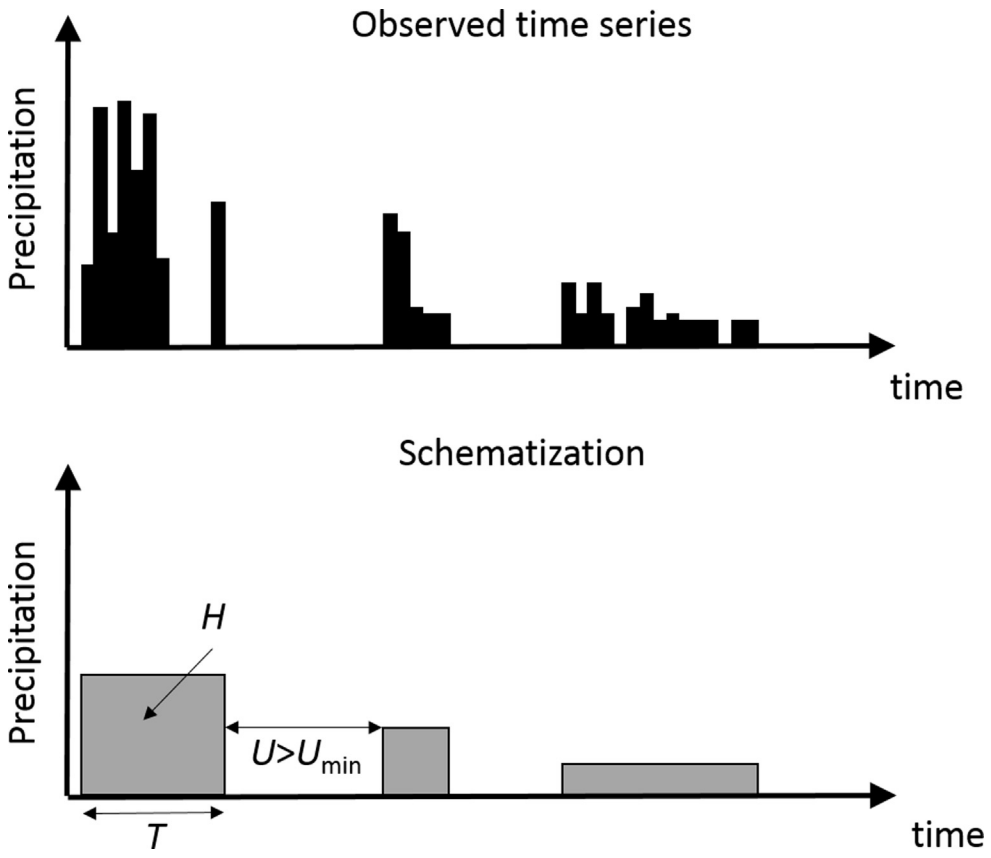

Fig. 2. Schematic of the stochastic rainfall model. A given series of precipitation (observed or from RCM simulations), is conceptualized as a sequence of rectangular rainfall events, separated by dry intervals. Each event is characterized by its duration T and total depth H (or, equivalently, by its mean intensity $I = H/T$), as well as the interarrival time from the preceding event $U > U_{min}$. Event duration and total depth are extracted from a bivariate distribution derived by copula modeling, while an independent univariate distribution is used to generate interarrival times.

function of antecedent rainfall, as introduced in our previous work (Peres and Cancelliere, 2014). The model which we briefly describe below, is partially implemented within the TRIGRS software, from the first version (Baum et al., 2002) to its updates (Baum et al., 2008; Alvioli and Baum, 2016). We have coded in MATLAB an ad hoc simplified implementation of this model. The simplification consists in the direct computation of the peak pressure head response to precipitation events, without calculation of the entire pressure head time history, which in the case of uniform hyetographs, is not necessary to determine whether or not a given event triggers a landslide. Thus this allows a more efficient application than other implementations, because it avoids operations unnecessary for the purpose of this paper, that cannot be bypassed if the above cited programs are used.

The model conceptualizes the hillslope as a single-layered

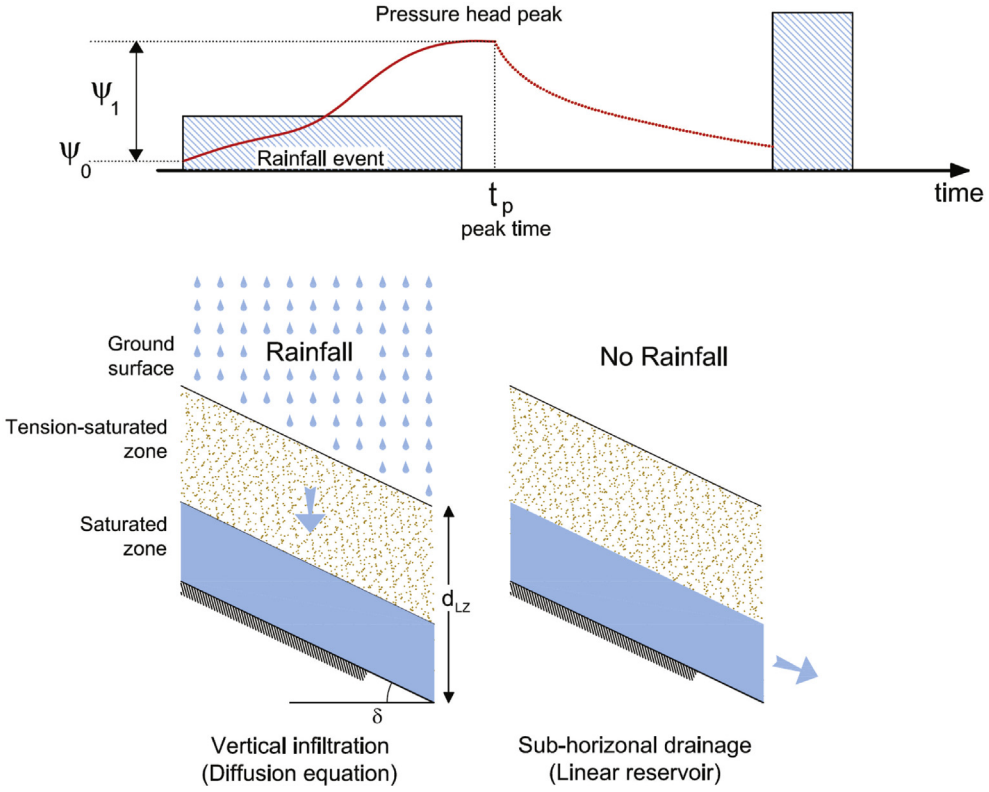

Fig. 3. Schematic of the hydrological model. Pressure head build-up during rainfall events, ψ_1, is modeled as a 1-D vertical infiltration process; drainage occurring in dry interarrivals is taken into account by a linear reservoir model, and determines porewater pressure at the beginning of each rainfall event (ψ_0). The maximum pressure head occurs at the base of soil layer. The factor of safety for slope stability is computed under the infinite slope hypothesis.

permeable strata overlaying a perfectly impermeable bedrock (Fig. 3).

As rainfall infiltrates, a saturated area develops above the regolith-bedrock interface, yielding an increase in pressure head, which negatively affects slope stability, according to Eq. (8). Within this scheme, pressure head is maximum at the base of the soil strata, which thus coincides with the failure plane. Hence, the aim of the hydrological model is to compute pressure head at the basal boundary ($Z = d_{LZ}$) and its local peak (occurring at time t_p from the beginning of any rainfall event).

Total pressure head ψ_i that builds in response at the i-th rainfall event is the sum of a transient $\psi_{1,i}$ and an initial component $\psi_{0,i}$:

$$\psi_i = \psi_{1,i} + \psi_{0,i} \tag{12}$$

The first part is modeled as a function of rainfall duration T and intensity I, while the initial pressure head for the i-th rainfall event depends on antecedent rainfall events; specifically, it is taken as function of the dry time interval before the event and the peak total pressure head of the preceding event ($i - 1$). The transient response is computed from the simplified form of the Richards' equation treated by Iverson (2000), which basically assumes that, with respect to the infiltration process, the unsaturated soil has the same hydrological properties of the saturated one (tension-saturated soil). Under these hypothesis, event pressure head component is given by (Baum et al., 2002, 2008):

$$\psi_1(d_{LZ}, t^*) = d_{LZ}\frac{I}{K_S}[R(t_p^*) - R(t_p^* - T^*)] \tag{13}$$

The response function $R(x)$ appearing in the above equation is given by a series of integral complementary error functions ierfc:

$$R(x) = 2\sum_{m=1}^{\infty} \text{ierfc}\left(\frac{2m-1}{\sqrt{x}}\right). \tag{14}$$

where

$$\text{ierfc}(x) = \frac{1}{\sqrt{\pi}}\exp(-x^2) - x\text{erfc}(x). \tag{15}$$

In the above equations, I and T are respectively rainfall event (mean) intensity and duration, K_S is the saturated hydraulic conductivity, D_0 is the soil saturated diffusivity, x is a dummy variate, and erfc is the complementary error function (Abramowitz and Stegun, 1964). In applying Eq. (13), two constraints have to be considered: first, the ratio I/K_S has to be truncated at 1 if greater, since K_S represents, for the model assumptions, the maximum possible value of the vertical infiltration rate; second, the so-called beta-line limitation that $\psi(d_{LZ}) \leqslant d_{LZ}\cos^2\delta$ applies, which is pressure head cannot exceed the value corresponding to an hydrostatic profile with water table located at the ground surface (Iverson, 2000). Dimensionless quantities in Eq. (13) are defined as follows:

$$t^* = \frac{t}{T_D}, \quad T^* = \frac{T}{T_D}\ T_D = \frac{d_{LZ}^2}{D}, \quad D = \frac{4D_0}{\cos^2\delta}, \tag{16}$$

The dimensionless peak time t_p^*, shown in Fig. 4 as a function of dimensionless rainfall event duration T^*, can be obtained from numerical investigation of Eqs. (13) and (14) (cf. D'Odorico et al., 2005).

Initial pressure head is here computed by the following equation (see Peres and Cancelliere, 2014):

$$\psi_{0,i} = \psi_{p,i-1}\exp\left(-\frac{u_i}{\tau_M}\right) \tag{17}$$

where $\psi_{p,i-1}$ is total pressure head at the peak time of t_p of preceding event $i - 1$, and u_i denotes the dry interval preceding current event i (see Fig. 2). The recession constant τ_M is here expressed as a function of a topographic wetness index, soil saturated hydraulic conductivity K_S, and porosity taken as the difference between saturated and residual soil water contents ($\theta_S - \theta_R$):

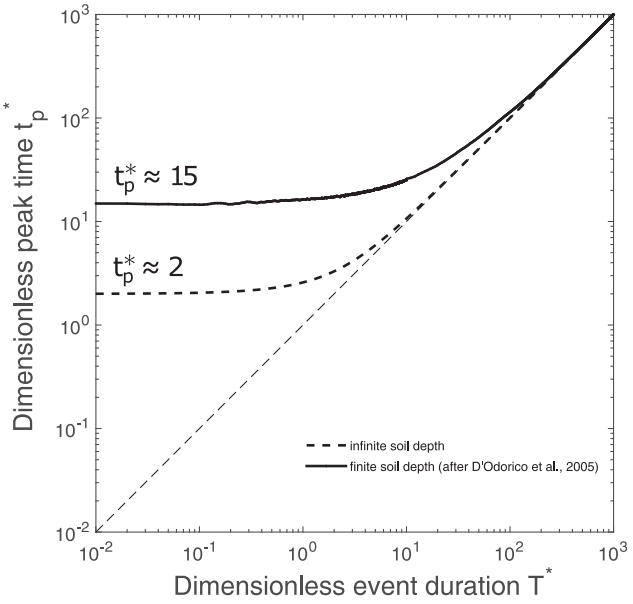

Fig. 4. Dimensionless peak time of pressure head as a function of dimensionless rainfall duration. The case of finite soil depth is compared to that of infinite (see D'Odorico et al., 2005).

$$\tau_M = \frac{(A/B)(\theta_S - \theta_R)}{K_S \sin\delta} \tag{18}$$

where A/B is the specific upslope contributing area, i.e. the ratio between the upslope contributing area A and contour length B. A/B can be computed according to various flow direction algorithms. Here the simple D8 method of O'Callaghan and Mark (1984) is used. Eq. (17) is a recursive equation that implicitly links initial pressure head to antecedent rainfall.

3. Application

3.1. Case study region: Peloritani mountains, Sicily, Italy

An application of the proposed methodology has been carried out with reference to the Peloritani Mountains region located in Northeastern Sicily, Italy, and represented in Fig. 5a. This highly landslide prone area has experienced several regional shallow landslide events; recent episodes are: 15 September 2006, 25 October 2007, 24 September 2009 and 1 October 2009 (see pictures in Fig. 5b–e). The latter event has caused severe damage and fatalities (37 deaths and thousands of evacuated people), and it has been described in several studies (Aronica et al., 2012; Peres and Cancelliere, 2012, 2014; De Guidi and Scudero, 2013; Lombardo et al., 2014; Cama et al., 2015; Schilirò et al., 2015, 2016; Stancanelli et al., 2017).

Table 1
Soil properties considered for application of the model to the Peloritani mountains case-study area (after Stancanelli et al., 2017).

ϕ' [°]	c' [kPa]	γ_s [N m^{-3}]	θ_S [–]	θ_R [–]	K_s [m s^{-1}]	D_0 [m^2 s^{-1}]	d_{LZ} [m]	A/B [m]	δ [°]
39	4	19000	0.35	0.045	2×10^{-5}	5×10^{-5}	2	10	40

Representative data for the Peloritani mountains are shown in Table 1. The use of a single set of soil properties for the Peloritani mountains area is an approximation, as these vary from point to point. The values used here are within the range of those obtained from some surveys in the area and have proven to be among the ones leading to a reasonable reproduction of the spatial distribution of landslides occurred on 1 October 2009 (Stancanelli et al., 2017). Spatial distribution and uncertainty of soil characteristics can play a crucial role on the model predictive ability (Anagnostopoulos et al., 2015), but modeling their impact is beyond the scope of this paper.

For calibration (and validation) of the stochastic rainfall model in the observational period, the hourly rainfall series of Fiumedinisi rain gauge has been used – location is shown in Fig. 5a. The series covers the period from 5 January 2002 to 23 February 2011 (about nine years). This period can be considered to be homogeneous to the control period (1971–2000), as several studies have shown the absence of significant trends in rainfall records covering a long period (from late 1920s to 2013) for both extreme and daily rainfall (Bonaccorso et al., 2005; Arnone et al., 2013; Bonaccorso and Aronica, 2016).

The following three RCM data sets of daily precipitation from the MED-CORDEX project (www.med-cordex.eu), having a spatial resolution of 0.44° (about 50 km), have been considered: (a) CMCC:

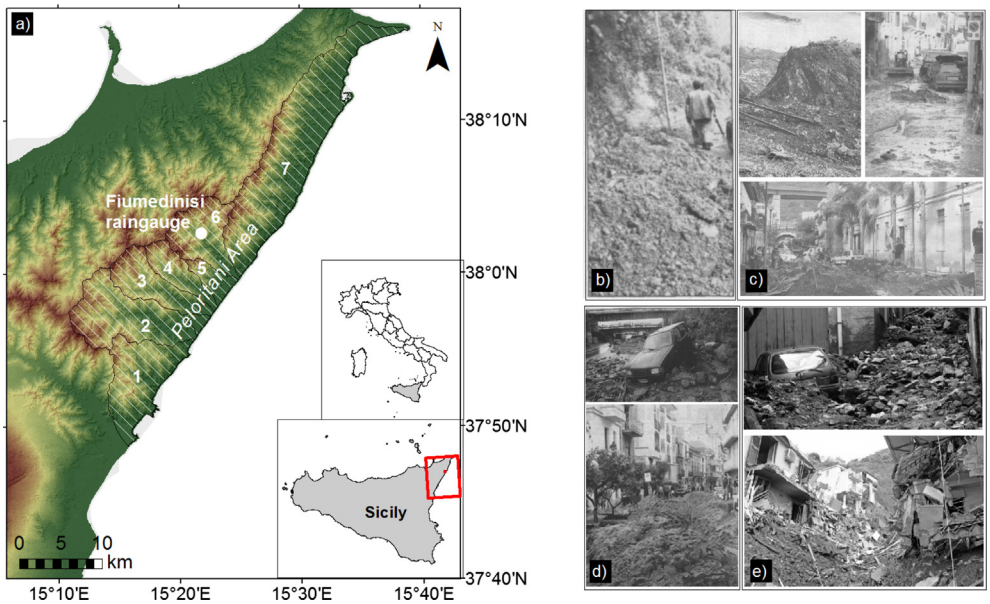

Fig. 5. Peloritani Mountains: (a) map of the area, showing elevation, main catchments, and location of the Fiumedinisi rain gauge; photographs of impacts of mass movements that occurred recently: (b) 15 September 2006, (c) 25 October 2007, (d) 24 September 2009, and (e) 1 October 2009.

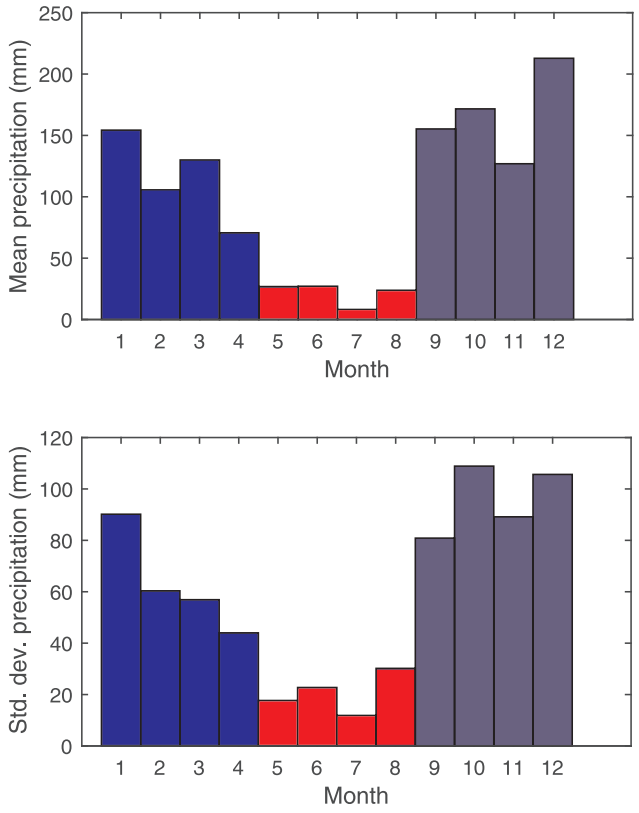

Fig. 6. Seasonal statistics of precipitation observed at Fiumedinisi rain gauge (mean and standard deviation of monthly total precipitation).

developed at the Mediterranean centre for climate change (Italy), it is based on CMCC-CCLM4-8-19 RCM applied to the CMCC-CM GCM; (b) GUF: developed ad the Goethe university Frankfurt (Germany), it is based on GUF-CCLM4-8-18 RCM applied to MPI-ESM-LR GCM; and (c) LMD: developed at the Laboratoire de météorologie dynamique (France), it is based on LMD-LMDZ4-NEMOMED8 RCM applied to the IPSL-CM5A-MR GCM. Spatial linear interpolation has been performed on the RCM data to derive the precipitation at the location of the Fiumedinisi rain gauge, as anticipated on Section 2.2.

3.2. Rainfall model calibration

The stochastic model takes into account seasonality of rainfall event characteristics, through separate calibrations for statistically homogeneous periods of the year, which have been identified based on the mean and standard deviation of monthly rainfall (See Fig. 6). Based on the plots, the following periods have been considered: (i) January – April (JFMA), (ii) May – August (MJJA), and (iii) September – December (SOND).

The observed rainfall hourly series has been then pre-processed to extract the rainfall events, which have been approximated as a constant-intensity hyetograph (see Fig. 2). A minimum event separation time interval U_{min} = 24 h has been chosen, following our previous studies (Peres and Cancelliere, 2014, 2016). Other researchers confirm the suitability of this value, as it has been used in determining landslide thresholds in Sicily (Caracciolo et al., 2017) and in Italy in general (Brunetti et al., 2010).

Among several tested distributions (Exponential, Weibull, Lognormal and Gamma), the Gamma resulted the most suitable for event duration, while a two-parameter Lognormal was suitable for both event depth and adjusted interarrival time $U' = U - U_{min}$. This last distribution is equivalent to a three-parameter Lognormal distribution with lower limit U_{min} (Matalas, 1963; Sangal and Biswas, 1970). Separate marginals have been fitted to the sub-datasets of each season. Formulas for parameter estimation by the MME for the specific marginal distributions used here are recalled for completeness in Appendix A. Fig. 7 shows a good fitting of the chosen marginals distributions in a Q-Q plot (comparison between observed and theoretical distribution-based quantiles).

The goodness-of-fit was also assessed by the Anderson-Darling statistical test (e.g. Kottegoda and Rosso, 2008), whose results are shown in Table 2, in terms of *p*-values, together with the estimated parameter values. *p*-values are defined as the probability that the test statistic could have been as extreme, or more extreme, than observed, if the null hypothesis (H_0: sample drawn from the fitted distribution) were true (cf. Upton and Cook, 2008). As can be seen from the table, the null hypothesis is not rejected with a level of significance greater than 5% for all variables and seasons, with the exception of rainfall duration in season MJJA for which the test is accepted with a 4% significance level. However, such a lower degree of fit for the MJJA season has minor consequences in assessing impacts of climate change on landslides, as in this season it is very unlikely for landslides to occur.

For modeling the dependence between rainfall event duration and total depth in each season, the best-fitting copula has been searched among the elliptical (Gaussian and Student'*st*) and Archimedean (Clayton, Gumbel, Frank, Joe, BB1, BB6, BB7, and BB8) families and the 90-, 180- and 270-degrees rotated versions, for a total of 32 copulas (which also include the independence one). The VineCopula R-Software has been used (Brechmann and Schepsmeier, 2013), which allows for selection of the most suitable copula among various hypothesized ones, based on Akaike Information Criteria (AIC) or Bayesian Information Criteria (BIC) – some additional details are summarized in Appendix A.

The following copulas resulted as the most suitable: Gaussian (JFMA), BB7 (MJJA), and survival Gumbel (SOND), for which essential details are given in Appendix A. Fig. 8 shows the comparison between observed and generated (H, T) pairs, as well as the parameters of the

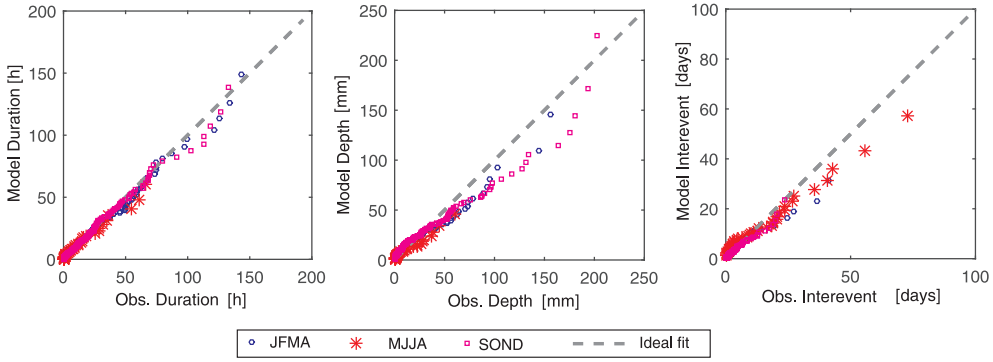

Fig. 7. Graphical goodness-of-fit (Q-Q plots) of the chosen marginal distributions for rainfall event characteristics: duration T (Gamma), depth H (Lognormal), and inter-arrival time U'. Specific markers and colors are associated to each season (JFMA, MJJA, and SOND).

Table 2
Univariate marginal distribution fit to rainfall characteristics for stochastic generation of rainfall event sequences. The *p*-values are relative to the Anderson-Darling goodness-of-fit test (null hypothesis H_0: sample can be considered as draw from the distribution). Commonly a *p*-value > 0.05 is taken to accept H_0.

Variable		Distribution	Season	β_1	β_2	*p*-value
Duration	T	Gamma(a, θ)	JFMA	0.80	34.11	0.22
		$\beta_1 = a$	MJJA	0.50	22.00	0.04
		$\beta_2 = \theta$	SOND	0.77	30.44	0.32
Depth	H	Logn (μ, σ)	JFMA	2.43	1.05	0.50
		$\beta_1 = \mu$	MJJA	1.60	1.07	0.61
		$\beta_2 = \sigma$	SOND	2.72	1.07	0.71
Interarrival	U'	Logn (μ, σ)	JFMA	0.70	1.15	0.56
		$\beta_1 = \mu$	MJJA	2.18	0.93	0.68
		$\beta_2 = \sigma$	SOND	0.58	1.03	0.80

fitted copulas. A good agreement can be seen, also in terms of the duration-intensity pair.

3.3. Model testing

In Fig. 9 a validation of the stochastic rainfall model, based on the comparison of observed and simulated yearly cumulative rainfall series is shown. The similarity (in a statistical sense) between the observed and simulated rainfall demonstrates the suitability of the stochastic rainfall model.

The suitability of the landslide model has been tested by checking its ability in spotting the dates of historical landslides when the observed rainfall series is given in input to it. The model indicates all and only the observed four landslides (Fig. 10), occurred on dates 15 September 2006, 25 October 2007, 24 September 2009 and 1 October 2009. We have also performed a sensitivity analysis relative to the choice of U_{min}, varying its value to 6, 12, 24, and 48 h. Except for the adopted value of 24 h, in all cases the test performed worse, in the sense

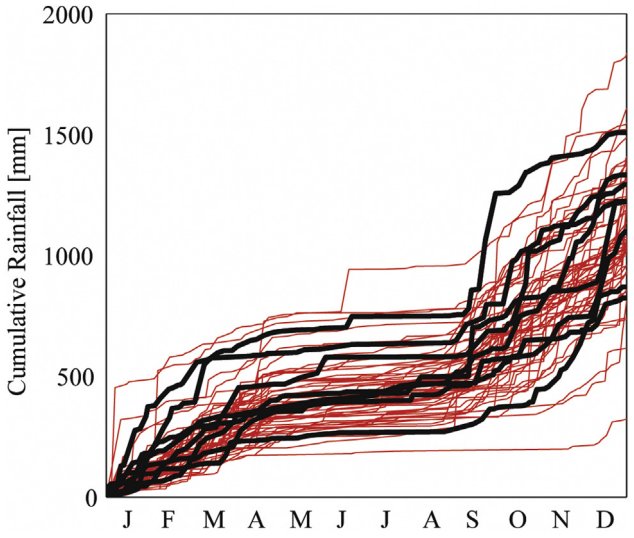

Fig. 9. Comparison between observed (thick black) and generated (red) yearly cumulative precipitation series. (For interpretation of the references to colour in this figure legend, the reader is referred to the web version of this article.)

that some landslide dates where not correctly spotted, and the count of critical pressure head exceedance was different from the number of observed landslides. This further validates the choice of U_{min} = 24 h.

An additional validation test has been conducted to check if the whole Monte Carlo modeling chain (rainfall plus hydrological and slope stability model) produces acceptable results for the purposes under study. To this aim, we have compared the number of landslides within the record with those given by the modeling chain on periods of the same length (9 years). This comparison cannot be done deterministically, because of sampling variability. Thus 30 simulations have been carried out. As can be seen from the boxplot of the results of these simulations, the model provides reasonable results, as a number of 4 landslides in nine years is within the interquartile range of the outcome of Monte Carlo simulations (see Fig. 11).

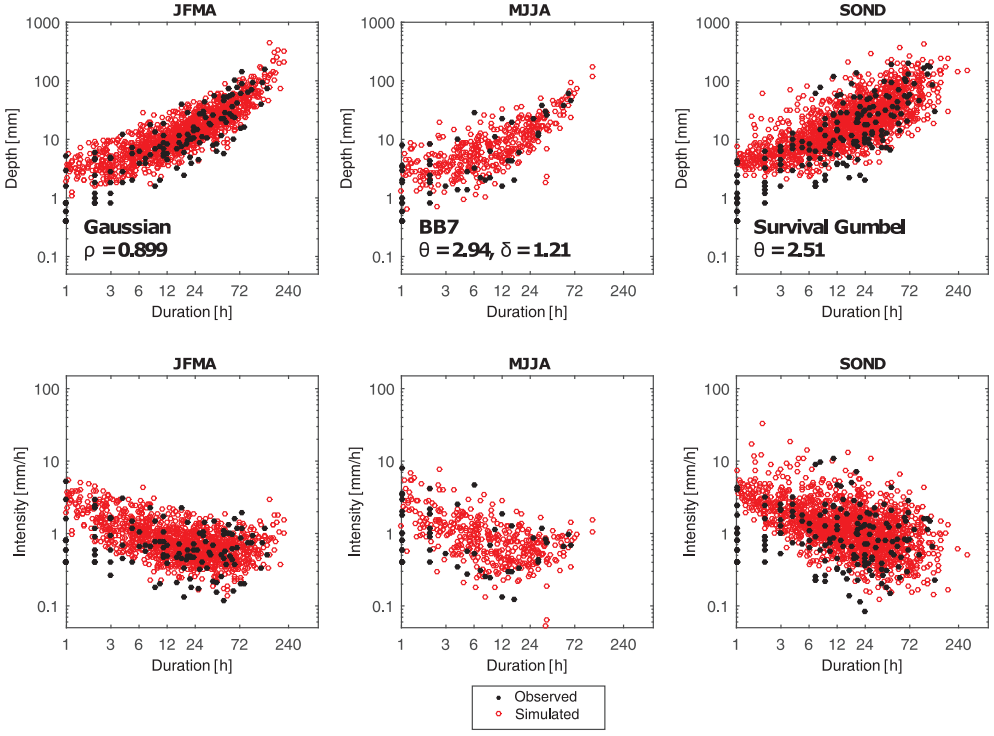

Fig. 8. Bivariate modeling of rainfall event duration and intensity by copula functions. Figure compares observed pairs with those generated randomly from the developed bivariate distribution. In the panels the copula parametric type and estimated values of the parameters are shown; each copula is relative to one season. The good agreement between observed and generated data demonstrates a good degree of fitting, and thus the suitability of the chosen copulas.

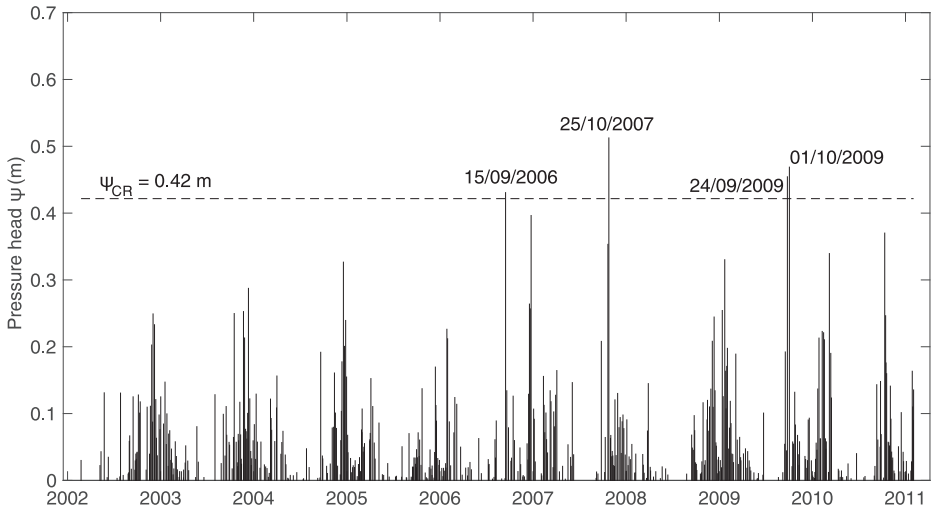

Fig. 10. Pressure head series obtained from observed rainfall data and the lumped hydrological model compared to the critical value. All and only the four events that have triggered landslides in the past yield a computed pressure head exceeding the critical value.

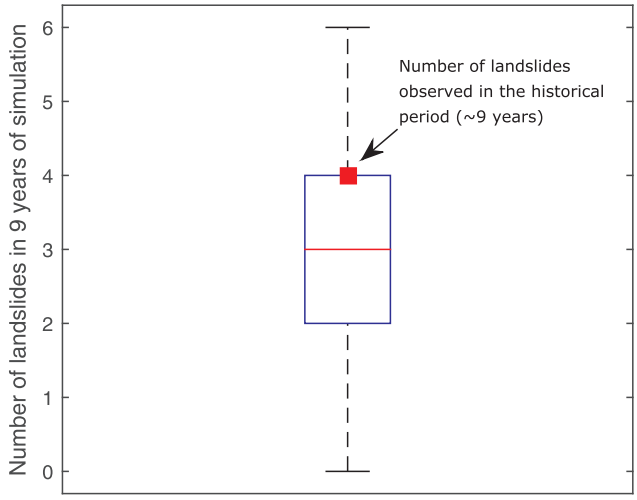

Fig. 11. Comparison of the number of landslides given by each Monte Carlo simulation with those observed in a period of the same length (9 years), showing that the observed series is one possible realization of the fitted stochastic model.

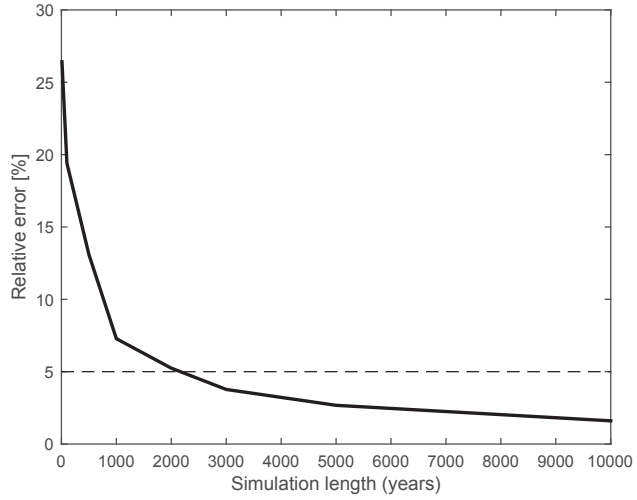

Fig. 12. Relative error in landslide return period estimation as a function of the simulation length.

Another point concerns the length of Monte Carlo simulations, that has to be sufficiently large to provide probability estimations of acceptable uncertainty (below a given tolerance, say 5%). A general overview of this problem is given in Kottegoda and Rosso (2008). Here we conduct sample variability in estimating landslide probability for the observed current climate (see Fig. 12). For every hypothetical value of the simulation length, M, landslide probability has been computed 30 times using the stochastic model calibrated on the observed series, operating a resampling from the generated events. This has enabled to compute the relative error in estimating landslide probability for each simulation length. More precisely, the relative error for a given simulation length is in this context defined as the ratio between the standard deviation and the mean of the landslide probability values obtained from the 30 samples. We have chosen a value of $M = 3000$ as it corresponds to a relative error in estimating landslide probability that is less than 5%.

4. Results and discussion

4.1. Changes in characteristics of rainfall events

Factors of changes for the moments of rainfall event characteristics (T, H and U), used to compute the adjusted rainfall generator parameters for years 2040–2100, are shown in Fig. 13.

The following changes, grouped per variable, may be inferred from the plots:

- Changes in duration T (Fig. 13a and b): In the RCP 4.5 scenario, changes of mean duration of events are quite low, either in the JFMA and the SOND season, while some significant changes are indicated in the MJJA season by the LMD projections for the period 2040–2060. Changes of standard deviation follow a very similar trajectory to those of the mean. In the RCP 8.5 scenario, changes are more accentuated compared to those in the RCP 4.5, and, for the JFMA and SOND seasons, projections indicate a slight decrease of event duration, which tends to become increasingly significant as the end of century is approached. However, these changes are quite limited (factor of change not less than 0.8). Again, changes of the standard deviation of rainfall event duration are similar, though greater, that those of the mean. Relatively high changes are projected for the MJJA season – factors of change approaching 2 (LMD) or 0.5 (GUF) – though these may have a low impact on landslide triggering probability, for the quite low intensities and durations of this season.

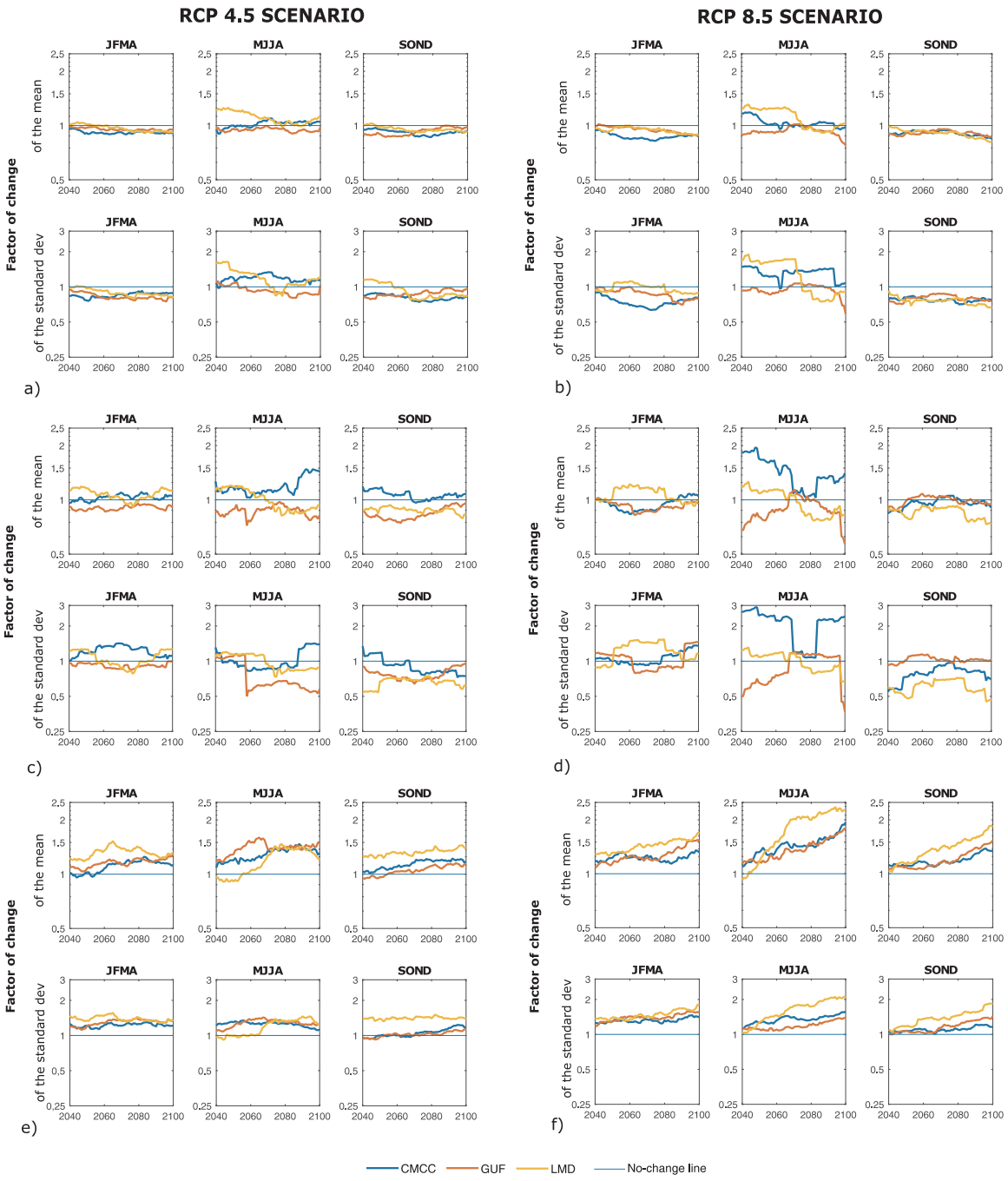

Fig. 13. Factor of changes in the two RCP scenarios, for mean and standard deviation of rainfall event duration T (a, b), depth H (c, d), and interevent time U (e, f).

- Changes for rainfall event depth H (Fig. 13c and d): Relatively to the RCP 4.5, factor of changes of mean rainfall event depth are comprised between 0.85 and 1.2 in the JFMA season, but centered around the no change line, while in the SOND season changes are more significant, with a prevailing indication of a decrease. Similarly to duration, in the MJJA season projected changes are more significant than in the other seasons (ranging from 0.7 to 1.5), but are quite unstable. Changes of standard deviation are again more significant than those of the mean, and prevalently indicate an increase of variability for rainfall event depth in the JFMA season, and an decrease in the SOND. For the RCP 8.5 scenario, changes are qualitatively similar than the RCP 4.5, but the factor of changes are in some cases more significant and unstable (cf. MJJA season).
- Changes in interarrival time U' (Fig. 13e and f): models concordantly indicate that the magnitude and variability of storm interarrival will tend to increase with time. A clear upward trend is predicted for the RCP 8.5 scenario, and factors of change can exceed 2 at the year 2100.

In general, with reference to rainfall duration and depth, the three considered RCMs provide indications that differ significantly from one to another, sometimes in opposite directions. On the other hand, models agree in predicting an increase of storm interarrival times, both in magnitude (mean) and variability (standard deviation), that becomes more significant moving forward in time. Also, all models predict some significant future changes of rainfall event depth mean and standard deviation in the SOND season (prevalently a decrease of both), the one where landslides have been more recurrent in the past (see Section 3.1).

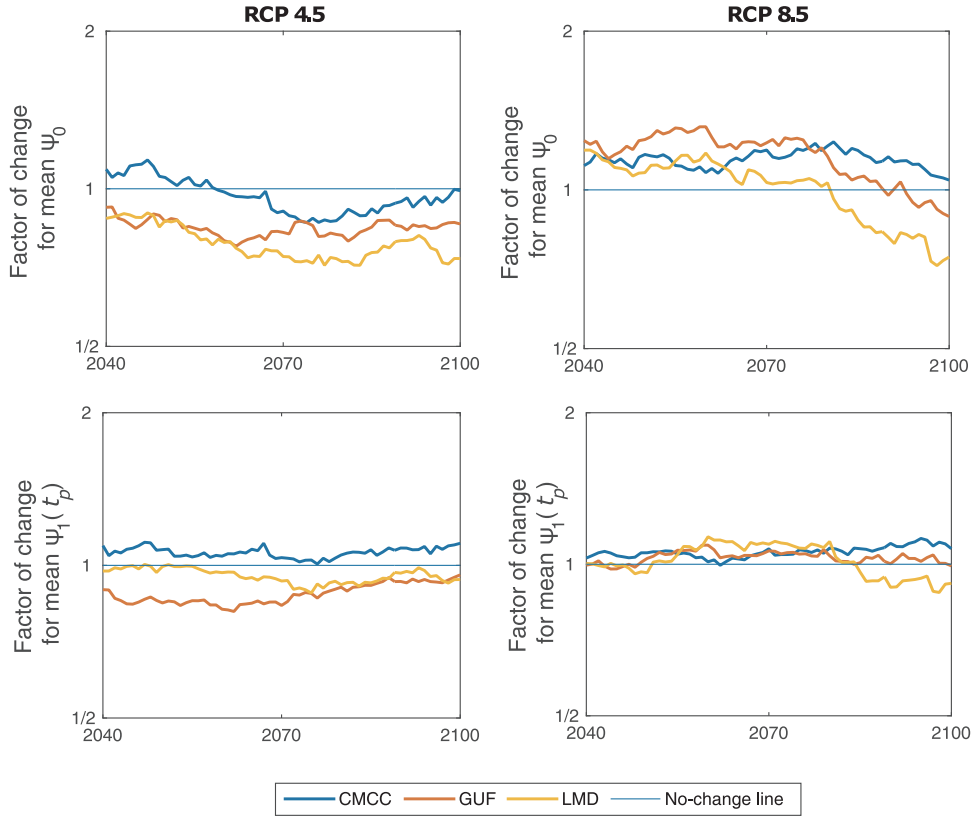

Fig. 14. Factor of changes for the mean of initial and peak transient pressure head, relatively to scenarios RCP 4.5 and RCP 8.5.

4.2. Changes in pressure head components and landslide return period

The obtained factors of changes have enabled us to perform Monte Carlo simulations for each future period. Fig. 14 shows the resulting factors of changes for the mean of initial ψ_0 and transient pressure head ψ_1 series (cf. Eq. (12)). As illustrated on Section 2.4, the first component is indirectly related to antecedent precipitation (Crozier, 1999), while the second is strictly dependent on the rainfall event intensity and duration characteristics. In the RCP 4.5 scenario there is an overall tendency for a decrease of initial pressure head. Only one RCM – the CMCC – indicates a possible slight increase, in the period 2040 –2060, with a factor of change not greater than 1.14. Also for the mean transient pressure head RCMs indicate prevalently a decrease. For the RCP 8.5 all RCM are concordant in indicating a negative trend of the changes of initial pressure head mean, though they remain positive until 2080 (LMD), ca 2090 (GUF), or on all the entire future period considered (CMCC). Changes of the mean transient pressure head are in this case very small, and can be deemed not significant (factor of change in the range 0.88 – 1.13).

The series of changes in landslide probability and return period are shown in Fig. 15.

For the RCP 4.5 scenario the models indicate in general a decrease of the probability of landslide triggering. In particular, models GUF and LMD show a decrease down to 1/4 respect to the baseline period. The CMCC model indicates an increase in the period 2040–2065, which is however quite small (less than 1.5). For the RCP 8.5 all three RCMs indicate a decrease of landslide probability, which is higher than for the previous scenario, being the factor of change $< 1/4$ in periods 2040–2050 and 2060–2100 (LMD model).

Changes in the return period are smoother than those in landslide probability, since Eq. (4) averages among the probabilities after any year at which return period is referred to. Return period has the opposite meaning of probability. Thus for RCP 4.5 models prevalently indicate a increase, with factors of change greater than 2 for the LMD and GUF models, while for the CMCC a slight decrease (> 0.70) is predicted in the initial period (2040–2060). For the RCP 8.5 the return period is projected to possibly increase to a greater factor than for RCP 4.5, with the highest values in period 2085–2100, where return period can be more than 3-times the current value (model LMD).

5. Conclusion

Estimation of landslide hazard is of key importance for land-use planning, and preparatory for landslide mitigation. As climate change is being claimed to potentially increase landslide activity, researchers and practitioners are nowadays asked to quantitatively assess the induced hazard changes. In our paper we have provided, tested and demonstrated a modeling chain methodology that allows the computation of future landslide return periods, taking into account of the non-stationarities in rainfall event characteristics induced by climate change. In particular, by sequential Monte Carlo simulations, the approach allows the estimation of the necessary sequence of landslide probabilities to apply formulas proposed by Salas and Obeysekera (2014) to compute return period under nonstationary climate conditions.

The tests and the application exercise conducted with reference to the Peloritani Mountains area, has demonstrated the capabilities of the proposed modeling approach, allowing also for a preliminary assessment of the possible future impacts of climate change on landslide hazard. According to the ensemble of the three MED-CORDEX RCMs considered, there will be a general tendency for a decrease of landslide hazard in the area, with return periods that can increase up to a factor of 2.5 or 3.5, respectively for RCP 4.5 and RCP 8.5. These results are a consequence of the projected increase of the interarrival time between rainfall events, combined with a prevalent decrease of rainfall event duration and depth. Only one model (the CMCC) projects, in certain periods, some slight increases of these rainfall event characteristics, and thus a decrease of return periods. Nevertheless, the relatively high

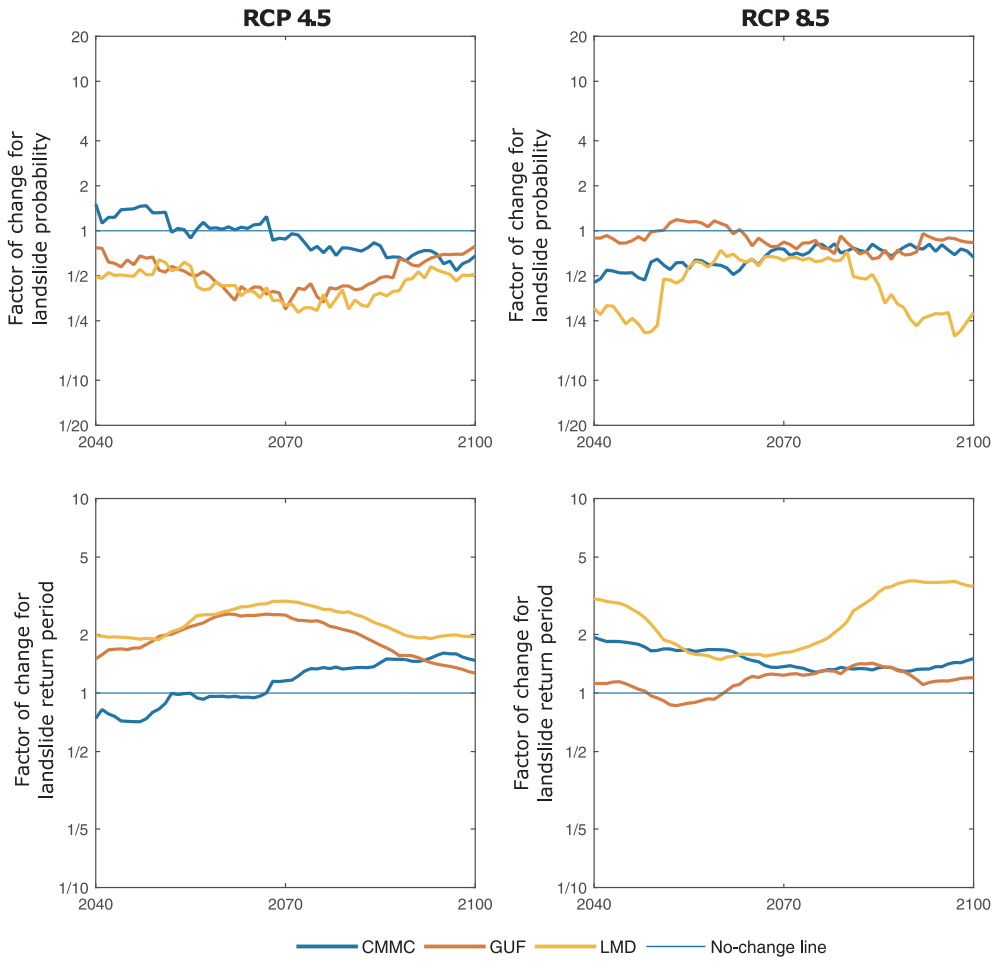

Fig. 15. Factor of changes for the non-exceedance probability and return period of landslide triggering, relatively to scenarios RCP 4.5 and RCP 8.5.

spread of the results due to climate modeling uncertainty, indicates the need for further research to confirm the specific results here obtained relatively to climate change impacts. This will be partially addressed in further research oriented to the use of a wider ensemble of RCM products – such as those provided under the EURO-CORDEX initiative (Jacob et al., 2014), as well as additional ones made available from the MED-CORDEX – also taking into account of their reliability by advanced ensemble averaging techniques (Christensen et al., 2010; Mascaro et al., 2018). Furthermore, the proposed approach is in principle suitable for many other areas with similar climatic, hydrological and geological conditions. The authors are willing to share the developed software tools with anyone interested to test the suitability of the modeling approach to other areas.

Acknowledgments

David J. Peres was supported by post-doctoral contract on “Studio dei processi idrologici relativi a frane superficiali in un contesto di cambiamenti climatici” (Analysis of landslide hydrological processes in a changing climate) funded by University of Catania. This research is also part of the program CLICHÉ - CLImate CHange and hydrological Extremes” of the Department of Civil Engineering and Architecture, University of Catania. The authors thank the two anonymous referees for their comments, which helped to considerably improve the paper.

Appendix A. Marginal distributions and copula models

For sake of clarity, the adopted marginal distributions and the copula functions used are shown below, along with some details on parameter estimation procedures.

The probability density function (pdf) of the Gamma distribution is:

$$f_X(x;a,\theta) = \frac{1}{\theta^a \Gamma(a)} x^{a-1} \exp(-x/\theta) \tag{A.1}$$

where X is the considered random variable (in our case, one of the following: rainfall event duration T, depth H or event interarrival time U), and x a specific value of X;a and θ are respectively the shape and the scale parameters, whose method-of-moments estimators (MME) are:

$$\hat{a} = \frac{n}{n-1}\frac{\bar{x}^2}{S^2} \tag{A.2}$$

$$\hat{\theta} = \frac{n-1}{n}\frac{S^2}{\bar{x}} \tag{A.3}$$

where $\bar{x} = \frac{\sum_{i=1}^{n} x_i}{n}$ and $S^2 = \frac{\sum_{i=1}^{n}(x_i - \bar{x})^2}{n-1}$ are the sample mean and sample variance, respectively, as x_i $i = 1, ..., n$ is the sample. For the Lognormal distribution expressions are:

$$f_X(x;\mu,\sigma) = \frac{1}{\sqrt{2\pi}x\sigma}\exp\left\{-\left(\frac{\log x - \mu}{\sigma}\right)\right\} \tag{A.4}$$

$$\hat{\mu} = \log\bar{x} - \frac{1}{2}\log\left(1 + \frac{S^2}{\bar{x}^2}\right) \tag{A.5}$$

$$\hat{\sigma} = \log\left(1 + \frac{S^2}{\bar{x}^2}\right) \tag{A.6}$$

Basic modeling with copulas is introduced in Nelsen (2007) and Genest and Favre (2007), and software tools are available under the open-source R statistical software (e.g. Brechmann and Schepsmeier, 2013).

The most suitable copulas for the stochastic rainfall model resulted to be (see Section 3.2): the Gaussian (season JFMA), the BB7 (MJJA), and the survival Gumbel (SOND). The Gaussian copula belongs to the elliptical family, and is given by:

$$C(x_1, x_2) = \Phi_\rho(\Phi^{-1}(x_1), \Phi^{-1}(x_2)) \tag{A.7}$$

where Φ_ρ denotes the bivariate standard normal distribution function with correlation parameter $-1 \leqslant \rho \leqslant 1$ and Φ^{-1} the inverse of the univariate standard normal distribution function. The BB7 and the Gumbel copulas belong to the Archimedean family, defined as

$$C(x_1, x_2) = \varphi^{[-1]}(\varphi(x_1) + \varphi(x_2)), \tag{A.8}$$

where φ: $[0, 1] \rightarrow [0, \infty]$ is a continuous strictly decreasing convex function such that $\varphi(1) = 0$ and $\varphi^{[-1]}$ is the pseudo-inverse

$$\varphi^{[-1]}(y) = \begin{cases} \varphi^{-1}(y), & 0 \leqslant y \leqslant \varphi(0) \\ 0 & \varphi(0) \leqslant y \leqslant \infty. \end{cases} \tag{A.9}$$

The generator function φ' defines specific copulas of this family, which, for the BB7 Copula (MJJA) and the Gumbel are respectively:

$$\varphi(\eta) = (1 - (1 - \eta)^{\omega})^{-\rho} - 1 \quad \text{with} \quad \omega \geqslant 1, \rho > 0, \tag{A.10}$$

and

$$\varphi(\eta) = (-\log\eta)^{\omega} \quad \text{with} \quad \omega \geqslant 1. \tag{A.11}$$

The Survival Gumbel copula is the Gumbel rotated by an angle of 180°, obtained as follows:

$$C_{180} = x_1 + x_2 - 1 + C(1 - x_1, 1 - x_2). \tag{A.12}$$

Parameters are estimated by pseudo maximum likelihood estimators, for which the reader is referred to Brechmann and Schepsmeier (2013).

Notation

GCM	global circulation model
RCM	regional climate model
RCP	representative concentration pathway
Y	first time a critical event occurs (r.v.)
p_0	probability of a given critical event
$f(y)$	mass probability function of Y
$\mathcal{T}_0 = 1/p_0$	return period (stationary)
$E(Y)$	expectation of Y
p_y	probability of a given critical event in year y (nonstationary)
t	dummy index
ν	future scenario year index
$\mathcal{T}_\nu$	return period at (future) year ν (nonstationary)
M	virtual length in years of a Monte Carlo simulation
m	virtual year of a Monte Carlo simulation
I_m	virtual landslide indicator function (Eq. (7))
F_S	factor of safety (slope stability)
ϕ' (effective)	friction angle
c' (effective)	cohesion
δ	terrain slope, measured from the horizontal direction
γ_s	soil unit weight
γ_w	unit weight of water
d_{LZ}	soil depth (vertical)
t_p	event pressure head response peak time
Z	vertical coordinate
ψ	pressure head
ψ_{CR}	critical pressure head
$\mathcal{F}_\nu$	factor of change for year ν
$\mathcal{M}$	statistical moment

T	rainfall event duration
H	rainfall event depth
$I = H/T$	rainfall event intensity
U	rainfall event interarrival
U_{min}	minimum interarrival time
$U' = U - U_{min}$	adjusted interarrival time
F_T	cumulative distribution function (cdf) for T
F_H	cdf for H
F_U	cdf for U
ψ_1	transient component of pressure head
ψ_0	initial component of pressure head
R	response function
D_0	saturated soil diffusivity
$\psi_{p,i-1}$	total pressure head at the peak time of preceding event
u_i	dry interval preceding current event i
τ_M	recession constant
θ_S	saturated soil water content
θ_R	residual soil water content
A	upslope contributing area
B	contour length
A/B	specific upslope contributing area (flow convergence)
f_X	probability density function of generic r.v. X
a, θ	parameters of a Gamma distribution
$\bar{x}$	sample mean
S^2	sample variance
n	sample size
μ, σ	parameters of a Lognormal distribution
η	dummy variate
C	copula function
C_{180}	180-degrees rotated copula
Φ_ρ	bivariate standard normal function with correlation parameter
φ	copula characteristic function
(x_1, x_2)	dummy two-dimensional variate
ω, ρ	parameters of generator function (copula)
Φ^{-1}	inverse of the univariate standard normal distribution
$\hat{\mu}$	estimate of μ

References

Abramowitz, M., Stegun, I.A., 1964. Handbook of Mathematical Functions: with Formulas, Graphs, and Mathematical Tables, vol. 55 Courier Corporation.

Alvioli, M., Baum, R., 2016. Parallelization of the TRIGRS model for rainfall-induced landslides using the message passing interface. Environ. Modell. Softw. 81, 122–135.

Alvioli, M., Melillo, M., Guzzetti, F., Rossi, M., Palazzi, E., von Hardenberg, J., Brunetti, M.T., Peruccacci, S., 2018. Implications of climate change on landslide hazard in Central Italy. Sci. Tot. Environ. 630, 1528–1543.

Anagnostopoulos, G.G., Fatichi, S., Burlando, P., 2015. An advanced process-based distributed model for the investigation of rainfall-induced landslides: the effect of process representation and boundary conditions. Water Resour. Res. 51 (9), 7501–7523.

Anandhi, A., Frei, A., Pierson, D.C., Schneiderman, E.M., Zion, M.S., Lounsbury, D., Matonse, A.H., 2011. Examination of change factor methodologies for climate change impact assessment. Water Resour. Res. 47 (3), 1–10.

Arnone, E., Noto, L., Lepore, C., Bras, R., 2011. Physically-based and distributed approach to analyze rainfall-triggered landslides at watershed scale. Geomorphology 133 (34), 121–131.

Arnone, E., Pumo, D., Viola, F., Noto, L., La Loggia, G., 2013. Rainfall statistics changes in Sicily. Hydrol. Earth Syst. Sci. 17 (7), 2449–2458.

Aronica, G., Brigandí, G., Morey, N., 2012. Flash floods and debris flow in the city area of Messina, north-east part of Sicily, Italy in October 2009: the case of the Giampilieri catchment. Nat. Hazards Earth Syst. Sci. 12 (5), 1295–1309.

Baum, R.L., Savage, W.Z., Godt, J.W., 2002. TRIGRS – A FORTRAN Program for Transient Rainfall Infiltration and Grid-Based Regional Slope-Stability Analysis. U.S. Geological Survey Open-File Report 02-0424, Reston, Virginia.

Baum, R.L., Savage, W.Z., Godt, J.W., 2008. TRIGRS – A FORTRAN program for transient rainfall infiltration and grid-based regional slope-stability analysis, version 2.0. U.S. Geological Survey Open-File Report 2008-1159, Reston, Virginia.

Baum, R.L., Godt, J.W., Savage, W.Z., 2010. Estimating the timing and location of shallow rainfall-induced landslides using a model for transient, unsaturated infiltration. J. Geophys. Res. 115, F03013.

Bellugi, D., Milledge, D.G., Dietrich, W.E., McKean, J.A., Perron, J.T., Sudderth, E.B., Kazian, B., 2015. A spectral clustering search algorithm for predicting shallow landslide size and location. J. Geophys. Res.: Earth Surface 120 (2), 300–324.

Bogaard, T., Greco, R., 2018. Invited perspectives: hydrological perspectives on precipitation intensity-duration thresholds for landslide initiation: proposing hydro-meteorological thresholds. Nat. Hazards Earth Syst. Sci. 18 (1), 31–39.

Bonaccorso, B., Aronica, G., 2016. Estimating temporal changes in extreme rainfall in Sicily Region (Italy). Water Resour. Manage. 30 (15), 5651–5670.

Bonaccorso, B., Cancelliere, A., Rossi, G., 2005. Detecting trends of extreme rainfall series in Sicily. Adv. Geosci. 2, 7–11.

Borga, M., Dalla Fontana, G., Cazorzi, F., 2002. Analysis of topographic and climatic control on rainfall-triggered shallow landsliding using a quasi-dynamic wetness index. J. Hydrol. 268 (1–4), 56–71.

Brechmann, E.C., Schepsmeier, U., 2013. Modeling dependence with C- and D-Vine copulas: the R Packatge CDVine. J. Stat. Softw. 52 (3), 1–27.

Brunetti, M.T., Peruccacci, S., Rossi, M., Luciani, S., Valigi, D., Guzzetti, F., 2010. Rainfall thresholds for the possible occurrence of landslides in Italy. Nat. Hazards Earth Syst. Sci. 10 (3), 447–458.

Caine, N., 1980. The rainfall intensity–duration control of shallow landslides and debris flows. Geogr. Ann. Ser. A Phys. Geogr. 62 (1/2), 23–27.

Callau Poduje, A.C., Haberlandt, U., 2017. Short time step continuous rainfall modeling and simulation of extreme events. J. Hydrol. 552, 182–197.

Cama, M., Lombardo, L., Conoscenti, C., Agnesi, V., Rotigliano, E., 2015. Predicting storm-triggered debris flow events: application to the 2009 Ionian Peloritan disaster (Sicily, Italy). Nat. Hazards Earth Syst. Sci. 15 (8), 1785–1806.

Cancelliere, A., 2017. Non stationary analysis of extreme events. Water Resour. Manage. 31 (10), 3097–3110.

Capparelli, G., Versace, P., 2014. Analysis of landslide triggering conditions in the Sarno area using a physically based model. Hydrol. Earth Syst. Sci. 18 (8), 3225–3237.

Caracciolo, D., Arnone, E., Conti, F.L., Noto, L.V., 2017. Exploiting historical rainfall and landslide data in a spatial database for the derivation of critical rainfall thresholds. Environ. Earth Sci. 76 (5), 222.

Chow, V.T., Maidment, D.R., Mays, L.W., 1988. Applied Hydrology. McGraw-Hill.

Christensen, J.H., Kjellström, E., Giorgi, F., Lenderink, G., Rummukainen, M., 2010. Weight assignment in regional climate models. Climate Res. 44, 179–194.
Ciabatta, L., Camici, S., Brocca, L., Ponziani, F., Stelluti, M., Berni, N., Moramarco, T., 2016. Assessing the impact of climate-change scenarios on landslide occurrence in Umbria Region, Italy. J. Hydrol. 541 (Part A), 285–295.
Coe, J.A., Godt, J.W., 2012. Review of approaches for assessing the impact of climate change on landslide hazards. In: In: Eberhardt, E., Froese, C., Turner, A., Leroueil, S. (Eds.), Landslides and Engineered Slopes, Protecting Society Through Improved Understanding, vol. 1. Taylor & Francis Group, London, pp. 371–377.
Crozier, M.J., 1999. Prediction of rainfall-triggered landslides: a test of the Antecedent Water Status Model. Earth Surf. Proc. Land. 24 (9), 825–833.
Crozier, M., 2010. Deciphering the effect of climate change on landslide activity: a review. Geomorphology 124 (3–4), 260–267.
D'Agostino, R.B., Stephens, M.A., 1986. Goodness-of-fit Techniques. M. Dekker.
De Guidi, G., Scudero, S., 2013. Landslide susceptibility assessment in the Peloritani Mts. (Sicily, Italy) and clues for tectonic control of relief processes. Nat. Hazards Earth Syst. Sci. 13 (4), 949–963.
De Michele, C., Salvadori, G., De Michele, C., 2003. A Generalized Pareto intensity-duration model of storm rainfall exploiting 2-Copulas. J. Geophys. Res. 108 (D2), 1–11.
D'Odorico, P., Fagherazzi, S., Rigon, R., 2005. Potential for landsliding: dependence on hyetograph characteristics. J. Geophys. Res.: Earth Surface 110, F01007.
Ehret, U., Zehe, E., Wulfmeyer, V., Warrach-Sagi, K., Liebert, J., 2012. HESS Opinions "Should we apply bias correction to global and regional climate model data?". Hydrol. Earth Syst. Sci. 16 (9), 3391–3404.
Evin, G., Favre, A.-C., 2008. A new rainfall model based on the Neyman-Scott process using cubic copulas. Water Resour. Res. 44 (3), W03433.
Fatichi, S., Ivanov, V.Y., Caporali, E., 2011. Simulation of future climate scenarios with a weather generator. Adv. Water Resources 34 (4), 448–467.
Froude, M.J., Petley, D.N., 2018. Global fatal landslide occurrence from 2004 to 2016. Nat. Hazards Earth Syst. Sci. 18 (8), 2161–2181.
Gariano, S., Guzzetti, F., 2016. Landslides in a changing climate. Earth Sci. Rev. 162, 227–252.
Gariano, S., Rianna, G., Petrucci, O., Guzzetti, F., 2017. Assessing future changes in the occurrence of rainfall-induced landslides at a regional scale. Sci. Tot. Environ. 417–426.
Genest, C., Favre, A.C., 2007. Everything you always wanted to know about copula modeling but were afraid to ask. J. Hydrol. Eng. 12 (4), 347–368.
Genest, C., Rémillard, B., Beaudoin, D., 2009. Goodness-of-fit tests for copulas: a review and a power study. Insurance: Math. Econ. 44 (2), 199–213.
Greco, R., Giorgio, M., Capparelli, G., Versace, P., 2013. Early warning of rainfall-induced landslides based on empirical mobility function predictor. Eng. Geol. 153, 68–79.
Guzzetti, F., Peruccacci, S., Rossi, M., Stark, C.P., 2007. Rainfall thresholds for the initiation of landslides in central and southern Europe. Meteorol. Atmos. Phys. 98, 239–267.
Guzzetti, F., Peruccacci, S., Rossi, M., Stark, C.P., 2008. The rainfall intensity-duration control of shallow landslides and debris flows: an update. Landslides 5 (1), 3–17.
Gyasi-Agyei, Y., Melching, C.S., 2012. Modelling the dependence and internal structure of storm events for continuous rainfall simulation. J. Hydrol. 249–261.
IPCC, 2014. Climate Change 2014: Synthesis Report. Contribution of Working Groups I, II and III to the Fifth Assessment Report of the Intergovernmental Panel on Climate Change. IPCC, Geneva, Switzerland p. 151.
Iverson, R.M., 2000. Landslide triggering by rain infiltration. Water Resour. Res. 36, 1897–1910.
Jacob, D., Petersen, J., Eggert, B., Alias, A., Christensen, O.B., Bouwer, L.M., Braun, A., Colette, A., Déqué, M., Georgievski, G., Georgopoulou, E., Gobiet, A., Menut, L., Nikulin, G., Haensler, A., Hempelmann, N., Jones, C., Keuler, K., Kovats, S., Kröner, N., Kotlarski, S., Kriegsmann, A., Martin, E., van Meijgaard, E., Moseley, C., Pfeifer, S., Preuschmann, S., Radermacher, C., Radtke, K., Rechid, D., Rounsevell, M., Samuelsson, P., Somot, S., Soussana, J.-F., Teichmann, C., Valentini, R., Vautard, R., Weber, B., Yiou, P., 2014. EURO-CORDEX: new high-resolution climate change projections for European impact research. Reg. Environ. Change 14 (2), 563–578.
Kilsby, C.G., Jones, P.D., Burton, A., Ford, A.C., Fowler, H.J., Harpham, C., James, P., Smith, A., Wilby, R.L., 2007. A daily weather generator for use in climate change studies. Environ. Modell. Softw. 22 (12), 1705–1719.
Kottegoda, N.T., Rosso, R., 2008. Applied Statistics for Civil and Environmental Engineers, second ed. Wiley-Blackwell.
Lehmann, P., Or, D., 2012. Hydromechanical triggering of landslides: from progressive local failures to mass release. Water Resour. Res. 48 (3).
Lombardo, L., Cama, M., Maerker, M., Rotigliano, E., 2014. A test of transferability for landslides susceptibility models under extreme climatic events: Application to the Messina 2009 disaster. Nat. Hazards 74 (3), 1951–1989.
Maraun, D., Wetterhall, F., Chandler, R.E., Kendon, E.J., Widmann, M., Brienen, S., Rust, H.W., Sauter, T., Themeßl, M., Venema, V.K.C., Chun, K.P., Goodess, C.M., Jones, R.G., Onof, C., Vrac, M., Thiele-Eich, I., 2010. Precipitation downscaling under climate change: recent developments to bridge the gap between dynamical models and the end user. Rev. Geophys. 48, 1–38.
Mascaro, G., Viola, F., Deidda, R., 2018. Evaluation of precipitation from EURO-CORDEX regional climate simulations in a small-scale mediterranean site. J. Geophys. Res.: Atmos. 123 (3), 1604–1625.
Matalas, N., 1963. Probability distribution of low flows. Geological Survey Professional Paper 434-A.
Melillo, M., Brunetti, M.T., Peruccacci, S., Gariano, S.L., Guzzetti, F., 2015. An algorithm for the objective reconstruction of rainfall events responsible for landslides. Landslides 12 (2), 311–320.
Melillo, M., Brunetti, M.T., Peruccacci, S., Gariano, S.L., Roccati, A., Guzzetti, F., 2018. A tool for the automatic calculation of rainfall thresholds for landslide occurrence. Environ. Modell. Softw. 105, 230–243.
Milledge, D.G., Bellugi, D., McKean, J.A., Densmore, A.L., Dietrich, W.E., 2014. A multidimensional stability model for predicting shallow landslide size and shape across landscapes. J. Geophys. Res.: Earth Surface 119 (11), 2481–2504.
Mood, A.M., Graybill, F.A., Boes, D.C., 1974. Introduction to the Theory of Statistics. McGraw-Hill.
Nelsen, R.B., 2007. An Introduction to Copulas, second ed. Springer Series in Statistics Springer, NY.
Obeysekera, J., Salas, J.D., 2016. Frequency of recurrent extremes under nonstationarity. J. Hydrol. Eng. 21 (5), 04016005.
O'Callaghan, J.F., Mark, D.M., 1984. The extraction of drainage networks from digital elevation data. Comput. Vis. Graphics Image Process. 28 (3), 323–344.
Peres, D.J., Cancelliere, A., 2012. Development of rainfall thresholds for landslide early warning in Sicily: a method based on the use of rainfall annual maxima series. Rendiconti Online Societa Geologica Italiana 21 (PART 1), 580–582.
Peres, D.J., Cancelliere, A., 2014. Derivation and evaluation of landslide-triggering thresholds by a Monte Carlo approach. Hydrol. Earth Syst. Sci. 18 (12), 4913–4931.
Peres, D.J., Cancelliere, A., 2016. Estimating return period of landslide triggering by Monte Carlo simulation. J. Hydrol. 541, 256–271.
Peres, D.J., Cancelliere, A., Greco, R., Bogaard, T., 2018. Influence of uncertain identification of triggering rainfall on the assessment of landslide early warning thresholds. Nat. Hazards Earth Syst. Sci. 18 (2).
Peruccacci, S., Brunetti, M.T., Gariano, S.L., Melillo, M., Rossi, M., Guzzetti, F., 2017. Rainfall thresholds for possible landslide occurrence in Italy. Geomorphology 290, 39–57.
Raia, S., Alvioli, M., Rossi, M., Baum, R.L., Godt, J.W., Guzzetti, F., 2014. Improving predictive power of physically based rainfall-induced shallow landslide models: a probabilistic approach. Geosci. Model Dev. 7 (2), 495–514.
Reid, M.E., Christian, S.B., Brien, D.L., Henderson, S.T., 2015. Scoops3D: software to analyze 3D slope stability throughout a digital landscape. U.S. Geological Survey, USGS Publications Warehouse,Techniques and Methods 14-A1, Reston, Virginia.
Rianna, G., Comegna, L., Mercogliano, P., Picarelli, L., 2016. Potential effects of climate changes on soil-atmosphere interaction and landslide hazard. Nat. Hazards 84 (2), 1487–1499.
Rosso, R., Rulli, M.C., Vannucchi, G., 2006. A physically based model for the hydrologic control on shallow landsliding. Water Resour. Res. 42 (6), 1–16.
Salas, J.D., 1993. Analysis and Modeling of Hydrologic Time Series. McGraw-Hill Ch. 19, Handbook of Hydrology.
Salas, J., Obeysekera, J., 2014. Revisiting the concepts of return period and risk for nonstationary hydrologic extreme events. J. Hydrol. Eng. 19 (3), 554–568.
Salciarini, D., Godt, J.W., Savage, W.Z., Baum, R.L., Conversini, P., 2008. Modeling landslide recurrence in Seattle, Washington, USA. Eng. Geol. 102 (3–4), 227–237.
Sangal, B.P., Biswas, A.K., 1970. The 3-parameter lognormal distribution and its applications in hydrology. Water Resour. Res. 6 (2), 505–515.
Schilirò, L., Esposito, C., Scarascia Mugnozza, G., 2015. Evaluation of shallow landslide-triggering scenarios through a physically based approach: an example of application in the southern Messina area (northeastern Sicily, Italy). Nat. Hazards Earth Syst. Sci. 15 (9), 2091–2109.
Schilirò, L., Montrasio, L., Scarascia Mugnozza, G., 2016. Prediction of shallow landslide occurrence: validation of a physically-based approach through a real case study. Sci. Tot. Environ. 134–144.
Seneviratne, S.I., Nicholls, N., Easterling, D., Goodess, C.M., Kanae, S., Kossin, J., Luo, Y., Marengo, J., McInnes, K., Rahimi, M., Reichstein, M., Sorteberg, A., Vera, C., Zhang, X., Rusticucci, M., Semenov, V., Alexander, L., Allen, S., Benito, G., Cavazos, T., Clague, J., Conway, D., Della-Marta, P., Gerber, M., Gong, S., Goswami, B., Hemer, M., Huggel, C., van den Hurk, B., Kharin, V., Kitoh, A., Tank, A., Li, G., Mason, S., McGuire, W., van Oldenborgh, G., Orlowsky, B., Smith, S., Thiaw, W., Velegrakis, A., Yiou, P., Zhang, T., Zhou, T., Zwiers, F., 2012. Changes in climate extremes and their impacts on the natural physical environment. In: Field, C., Barros, V., Stocker, T., Dahe, Q. (Eds.), Managing the Risks of Extreme Events and Disasters to Advance Climate Change Adaptation: Special Report of the Intergovernmental Panel on Climate Change. Cambridge University Press, Cambridge, pp. 109230 Ch. 3.
Sidle, R., Ochiai, H., 2006. Landslides: processes, prediction, and land use. Water resources monograph. Vol. 18. Americal Goephisical Union, 312p.
Simoni, S., Zanotti, F.F., Bertoldi, G., Rigon, R., 2008. Modelling the probability of occurrence of shallow landslides and channelized debris flows using GEOtop-FS. Hydrol. Processes 22, 532–545.
Stancanelli, L., Peres, D., Cancelliere, A., Foti, E., 2017. A combined triggering-propagation modeling approach for the assessment of rainfall induced debris flow susceptibility. J. Hydrol. 550.
Tarolli, P., Borga, M., Chang, K.T., Chiang, S.H., 2011. Modeling shallow landsliding susceptibility by incorporating heavy rainfall statistical properties. Geomorphology 133 (3-4), 199–211.
Taylor, K.E., Stouffer, R.J., Meehl, G.A., 2012. An overview of CMIP5 and the experiment design. Bull. Am. Meteorol. Soc. 93 (4), 485–498.
Teutschbein, C., Seibert, J., 2012. Bias correction of regional climate model simulations for hydrological climate-change impact studies: review and evaluation of different methods. J. Hydrol. 12–29.
Upton, G., Cook, I., 2008. A Dictionary of Statistics, second ed. Oxford Quick Reference Oxford University Press.
Vernieuwe, H., Vandenberghe, S., De Baets, B., Verhoest, N.E.C., 2015. A continuous rainfall model based on vine copulas. Hydrol. Earth Syst. Sci. 19 (6), 2685–2699.
Vessia, G., Parise, M., Brunetti, M.T., Peruccacci, S., Rossi, M., Vennari, C., Guzzetti, F., 2014. Automated reconstruction of rainfall events responsible for shallow landslides. Nat. Hazards Earth Syst. Sci. 14 (9), 2399–2408.